JOURNAL OF MATERIALS SCIENCE 28 (1993) 1–8

Influence of bending–twisting and extension–bending coupling on damping of laminated composites

S. J. HWANG, R. F. GIBSON
Wayne State University, Department of Mechanical Engineering, Advanced Composites Research Laboratory, Detroit, MI 48202, USA

This paper describes a three-dimensional finite element–strain energy method for characterizing vibration coupling effects on damping of laminated composites. The analysis was performed on graphite–epoxy laminated cantilever beams in two stacking sequences: (i) 12-ply symmetric laminates [12(θ)], and (ii) 12-ply antisymmetric laminates [6(θ)/6(− θ)]. Thus, the effects of vibration coupling between bending and twisting in symmetric laminates, and between extension and bending in antisymmetric laminates on damping were studied. A modal strain energy method was applied in a finite-element formulation to solve for the natural frequencies, mode shapes and energy dissipation of the laminates. The coupling energy dissipation was separated from the non-coupling energy dissipation by the decomposition of the total energy dissipation in order to study its contribution to damping. The results of the first three modes, which includes two flexural modes and one torsional mode, are presented. The resulting torsional damping data are generally higher than the flexural damping data. The coupling effects on damping in flexural modes were found to be more significant than those in torsional modes, and such effects appear to be dependent upon the fibre angle and the vibration mode of interest. The coupling effects appear to increase damping in flexural modes, and were found to be maximized at a fibre angle around 30°. The non-coupling energy dissipation was found to be more dominant for the flexural modes at a fibre angle of 90°, and it appears to be more dominant at a fibre angle of 0° in torsional modes, however.

1. Introduction

There are a number of possible coupling modes of interest in vibrating composite structures. One of the major coupling modes in symmetric composite laminates is the coupling between bending and twisting. The coupling between bending and extension (or bending-membrane), however, would only be present in non-symmetric laminates. So far, the effects of vibration coupling on natural frequencies and mode shapes have received much attention in the design and control of composite materials and structures [1–5]. For example, Pryor and Barker [1] used a finite element method to study the effect of bending–extensional coupling on the elastostatic behaviour of angle-ply laminated composites. Abarcar and Cunniff [2] investigated the effect of bending–twisting coupling on frequencies and mode shapes of symmetric composite laminates. On the other hand, the combined effect of bending–extensional and bending–twisting coupling on frequencies of non-symmetric composite laminates has been studied by Thornton and Clary [3]. They concluded that the combined coupling effects are such that they reduce bending stiffness and lower natural frequencies. Although considerable advances have been previously achieved in the analysis of vibration coupling on frequencies and mode shapes of advanced composite structures, the coresponding effects on damping and the cause of such effects have not been fully investigated. This paper describes a particular method for characterizing the effects of vibration coupling on damping of laminated composites.

Previous work in the area of damping analysis that appears to be relevant to our current work was the work by Adams and Bacon [6]. They used a strain energy method in a two-dimensional static analysis to study the effects of fibre orientation and laminate geometry on the flexural and torsional damping of fibre-reinforced composites. However, no attempt was made to investigate the contribution of coupling energy dissipation to damping. Related work by Lin *et al.* [7] and Adams and Lambert [8] also involved the use of the strain energy method in characterizing damping of composite materials, but the effects of vibration coupling were not considered.

The current analysis of damping is based on a previously developed strain energy method [9–14]. This method has recently been applied in the characterization of coupling effects on damping of symmetric composites, and only the results of the first flexural mode of vibration were reported [15, 16]. The strain

0022–2461

energy method was implemented in a three-dimensional finite element formulation to carry out the calculations of strain energy, coupling energy dissipation and damping. The advantage of this method is that the effects of three-dimensional states of stress are considered in the analysis of damping. Thus, the energy dissipation due to each of the six stress components (three in-plane stresses σ_x, σ_y and τ_{xy}, and three interlaminar stresses σ_z, τ_{xz} and τ_{yz}) can be decomposed from the total energy dissipation. The contribution of damping due to each of the six resulting stress components can then be found by taking the ratio of energy dissipation due to each of the six stress components to the total energy dissipation of the composite [10]. However, in order to investigate the contribution of coupling energy dissipation to the total laminate damping, further decomposition of the resulting six energy dissipation terms was required, as demonstrated in this paper. The method presented here was designed for general application in dealing with all associated coupling modes in any laminated material or structure.

The principal objectives of this paper are to describe the method for decomposing coupling energy dissipation and to characterize its effects on damping of laminated composites. The technique described here was based on modifications of a previous development, which involves the decomposition of energy dissipation for the purpose of identifying the coupling energy dissipation of interest [15, 16]. In particular, a three-dimensional finite element analysis was performed for the evaluation of resonant frequencies and mode shapes. The strain energy method was then implemented in a finite element formulation to evaluate the composite damping based on the resulting mode shapes and damping properties of the individual layers. Thus, the effects of all three-dimensional states of stress, especially interlaminar shear stresses, were included in the analysis [11, 12]. The effects of coupling on damping were finally examined by decomposing the energy dissipation attributed to the coupling energy dissipation components of interest. The results presented here were based on the first three modes of vibration, including two flexural modes and one torsional mode.

2. Coupling stiffnesses

Before starting the analysis of vibration coupling effects on damping of laminated composites, it is necessary to understand the relations between lamina and laminate coupling stiffnesses. The well-known classical lamination theory is derived based on a two-dimensional, plane-stress analysis, and only in-plane forces and moments are considered. Accordingly, for laminates consisting of multiple generally orthotropic laminae, the resulting forces and moments in a laminate can be expressed as functions of lamina strains, curvatures and the associated laminate stiffnesses, which are usually written in a shortened form [17]

$$\begin{bmatrix} N \\ M \end{bmatrix} = \begin{bmatrix} A & B \\ B & D \end{bmatrix} \begin{bmatrix} \varepsilon \\ \varkappa \end{bmatrix} \tag{1}$$

where A, B and D are extensional, coupling and bending stiffness matrices of the laminate, respectively. These laminate stiffnesses can be related to lamina stiffnesses by the following equations:

$$A_{ij} = \sum_{k=1}^{n} (\bar{Q}_{ij})^{(k)} (z_k - z_{k-1}) \tag{2}$$

$$B_{ij} = \sum_{k=1}^{n} (\bar{Q}_{ij})^{(k)} \frac{(z_k^2 - z_{k-1}^2)}{2} \tag{3}$$

$$D_{ij} = \sum_{k=1}^{n} (\bar{Q}_{ij})^{(k)} \frac{(z_k^3 - z_{k-1}^3)}{3} \tag{4}$$

where $(\bar{Q}_{ij})^{(k)}$ is the transformed reduced stiffnesses of the kth lamina [14], z is the laminate thickness coordinate, k is the lamina number, n is the total number of laminae and $i, j = 1, 2, 6$ (for two-dimensional plane stress analysis).

In this work, the graphite–epoxy composite laminates were analysed in two reinforcement configurations: (i) $[12(\theta)]$ symmetric laminates, and (ii) $[6(\theta)/6(-\theta)]$ antisymmetric laminates. Since the first model was a symmetric laminate, $B_{ij} = 0$ and all the elements in the A and D matrices would be present because of couplings between bending and twisting. Such coupling is evidenced by the presence of laminate coupling stiffnesses A_{16} and D_{16}. For the case of non-symmetric laminates, the B_{ij} are not necessarily equal to zero and the coupling stiffnesses A_{16} and D_{16} may not exist. For example, since the second model used in this work was an antisymmetric laminate, and because the laminate was made of an even number of laminae (12 plies), the coupling stiffness B_{16} exists, but A_{16} and D_{16} are both equal to zero.

Since the classical lamination theory neglects the interlaminar forces and moments, inaccurate results are always present in such an analysis of mechanical properties of composite materials. The current damping analysis, however, is based on a three-dimensional finite element analysis which includes all three-dimensional stresses and strains. It is therefore convenient to deal with a simpler but equivalent system of stresses and strains. The three-dimensional constitutive stress–strain relations for a linear elastic orthotropic lamina in non-principal coordinate directions x, y, z (where z is perpendicular to the laminate) are generally written in a shortened form as

$$\sigma^{(k)} = C^{(k)} \varepsilon^{(k)} \tag{5}$$

where $\sigma^{(k)}$ is the stress matrix of the kth lamina, $\varepsilon^{(k)}$ is the strain matrix of the kth lamina and $C^{(k)}$ is the transformed reduced stiffness matrix of the kth lamina.

For a generally orthotropic lamina with a non-zero fibre orientation, the C matrix contains 20 non-zero elements ($\bar{C}_{ij}$, where $i, j = 1, 2, 3, 4, 5, 6$), 6×6 matrix for a three-dimensional analysis [17]). For the case of two-dimensional analysis, C is a 3×3 matrix ($\bar{C}_{ij}$, where $i, j = 1, 2, 6$), and $\bar{C}_{ij} = \bar{Q}_{ij}$ as shown in Equations 2–4. Since laminate stiffnesses such as A_{ij}, B_{ij} and D_{ij} are derived from the lamina stiffnesses $\bar{Q}_{ij}$, a combined effect of laminate coupling stiffnesses A_{16}, B_{16} and D_{16} can be characterized by lamina coupling stiffnesses $\bar{Q}_{16}$ (or $\bar{C}_{16}$), lamina thickness, and laminate stacking sequence. The effect of lamina coupling

stiffness $\bar{Q}_{26}$ (or $\bar{C}_{26}$), which characterizes coupling between the bending in the lamina width direction and the in-plane twisting, is trivial for composite beams, and would be more important for the case of composite plates. The models analysed here were based on composite beams, and the coupling effects would be dominated by $\bar{C}_{16}$.

Accordingly, the combined effect of laminate coupling stiffnesses A_{16}, B_{16} and D_{16} on damping can be studied by calculating the coupling energy dissipation contributed by the corresponding lamina coupling stiffness $\bar{C}_{16}$. For example, $\bar{C}_{16}$ can be used to characterize A_{16} and D_{16} in symmetric laminates, since $B_{16} = 0$. For the case of antisymmetric laminates with an even number of plies, $\bar{C}_{16}$ can be used to characterize laminate coupling stiffness B_{16}, since both A_{16} and D_{16} are equal to zero. The work presented here was based on a three-dimensional analysis, and the 20 non-zero lamina stiffnesses ($\bar{C}_{ij}$) were used to calculate strain energy. The total strain energy of a laminate was calculated by summing strain energy stored in each lamina based on the resulting lamina stress and strain distributions, and was decomposed into 20 strain energy terms, including the coupling strain energy associated with the lamina coupling stiffness $\bar{C}_{16}$.

3. Strain energy/damping analysis

In the recent past, the strain energy method has been widely used in the characterization of damping of composite materials at both micromechanical and macromechanical levels [9–16]. The motivation for this work was to utilize the strain energy method in a finite element form to facilitate the analysis of vibration coupling effects on damping of laminated composites. We have previously developed a three-dimensional strain energy/damping equation for the prediction of damping of laminated composites [10–12]. The basis of this equation (Equation 6 below) is that the laminate loss factor (or damping) can be calculated by summing the energy dissipation in a composite laminate and dividing by the total strain energy stored in the laminate:

$$\eta = \sum_{k=1}^{n} [\eta_x^{(k)} W_x^{(k)} + \eta_y^{(k)} W_y^{(k)} + \eta_{xy}^{(k)} W_{xy}^{(k)} + \eta_z^{(k)} W_z^{(k)} + \eta_{yz}^{(k)} W_{yz}^{(k)} + \eta_{xz}^{(k)} W_{xz}^{(k)}]/W_t \quad (6)$$

where η is the laminate loss factor (a measure of damping), k is the lamina number, n is the total number of laminae, W_t is the total strain energy stored in a laminate at maximum displacement, $\eta_x^{(k)}$, $\eta_y^{(k)}$, $\eta_{xy}^{(k)}$ are in-plane loss factors of the kth lamina, $\eta_z^{(k)}$, $\eta_{yz}^{(k)}$, $\eta_{xz}^{(k)}$ are interlaminar loss factors of the kth lamina, $W_x^{(k)}$, $W_y^{(k)}$, $W_{xy}^{(k)}$ are in-plane strain energy terms of the kth lamina, and $W_z^{(k)}$, $W_{yz}^{(k)}$, $W_{xz}^{(k)}$ are interlaminar strain energy terms of the kth lamina.

The lamina in-plane loss factors were determined by the use of a micromechanical analysis, which involved the use of the elastic–viscoelastic correspondence principle and the transformation equations of complex moduli for off-axis fibres along non-principal material directions [18, 19]. Accordingly, the in-plane loss factors of a composite lamina can be expressed in terms of the corresponding constituent material properties. The resultant equations of the lamina in-plane loss factors are too long to be presented here. For a complete description of these micromechanical equations, the reader is referred to the references cited [18, 19]. Furthermore, since the matrix material is the bonding agent between two adjacent laminae, it is believed that the interlaminar energy dissipation is dominated by the matrix materials [10, 19]. For this reason, and because no micromechanical theory was available for the prediction of the lamina interlaminar loss factors, the matrix loss factors were used as the lamina interlaminar loss factors to simplify the solution. In this work, the matrix loss factors were measured by the use of an impulse-frequency response technique [18, 19].

One of the advantages of the strain energy method is that the contribution of damping due to each of the six resulting stress components can be investigated by calculating the energy dissipation due to each of the components [10–12]. In this work, it was found that only the longitudinal normal stress σ_x, in-plane shear stress τ_{xy} and the interlaminar shear stress τ_{xz} contributed significantly to the total energy dissipation. This is because the total strain energy is dominated by these three major stresses. It should be mentioned that, although the effects of σ_y, σ_z and τ_{yz} are trivial, their contribution to the total energy dissipation was included in the calculation of the total laminate damping as shown in Equation 6.

The strain energy corresponding to each of the three major stresses can be calculated based on the following equations

$$W_x^{(k)} = \tfrac{1}{2}\int \sigma_x^{(k)} \varepsilon_x^{(k)} \, dv = W_{x,x}^{(k)} + W_{x,y}^{(k)} + W_{x,z}^{(k)} + W_{x,xy}^{(k)} \quad (7)$$

$$W_{xy}^{(k)} = \tfrac{1}{2}\int \tau_{xy}^{(k)} \gamma_{xy}^{(k)} \, dv = W_{xy,x}^{(k)} + W_{xy,y}^{(k)} + W_{xy,z}^{(k)} + W_{xy,xy}^{(k)} \quad (8)$$

$$W_{xz}^{(k)} = \tfrac{1}{2}\int \tau_{xz}^{(k)} \gamma_{xz}^{(k)} \, dv = W_{xz,xz}^{(k)} + W_{xz,yz}^{(k)} \quad (9)$$

where W_x, W_{xy} and W_{xz} (with a superscript k) are the resulting three strain energy terms stored in the kth lamina due to σ_x, τ_{xy} and τ_{xz}, respectively, v is the volume of the kth lamina and $W_{x,x}$ etc. are strain energy terms defined later in Equations 10–13. The three major strain energy terms can be further decomposed into ten strain energy terms as given in Equations 7–9, which correspond to each of the associated non-zero elements of the lamina stiffness matrix. It was found that only five of the ten strain energy terms contributed greatly to the total strain energy for the laminates studied in this work. These five major strain energy terms consist of three non-coupling strain energy terms ($W_{x,x}$, $W_{xy,xy}$ and $W_{xz,xz}$) and two coupling strain energy terms ($W_{x,xy}$ and $W_{xy,x}$), and they are defined as

$$W_{x,x}^{(k)} = \tfrac{1}{2}\int [\bar{C}_{11}^{(k)} \varepsilon_x^{(k)}] \varepsilon_x^{(k)} \, dv \quad (10)$$

$$W^{(k)}_{xy,xy} = \tfrac{1}{2}\int [\bar{C}^{(k)}_{66}\,\gamma^{(k)}_{xy}]\gamma^{(k)}_{xy}\,dv \quad (11)$$

$$W^{(k)}_{xz,xz} = \tfrac{1}{2}\int [\bar{C}^{(k)}_{44}\,\gamma^{(k)}_{xz}]\gamma^{(k)}_{xz}\,dv \quad (12)$$

$$W^{(k)}_{x,xy} = \tfrac{1}{2}\int [\bar{C}^{(k)}_{16}\,\gamma^{(k)}_{xy}]\varepsilon^{(k)}_{x}\,dv = W^{(k)}_{xy,x} \quad (13)$$

It should be mentioned that $W_{x,xy} = W_{xy,x}$ (Equation 13), since the corresponding coupling stiffnesses are equal ($\bar{C}_{16} = \bar{C}_{61}$). Although $W_{x,xy} = W_{xy,x}$, this does not mean that coupling energy dissipation terms due to $\bar{C}_{16}$ and $\bar{C}_{61}$ are the same. This is because the lamina loss factors corresponding to the two coupling strain energy terms are different. The contribution of energy dissipation due to each of the three major stresses can be expressed as

$$F_x = D_x/D_t,\ F_{xy} = D_{xy}/D_t,\ F_{xz} = D_{xz}/D_t \quad (14)$$

where D_x, D_{xy}, D_{xz} are energy dissipation due to σ_x, τ_{xy} and τ_{xz}, respectively; F_x, F_{xy}, F_{xz} are fraction of damping due to σ_x, τ_{xy} and τ_{xz}, respectively; and D_t is the total energy dissipation in the laminate ($= \eta W_t$).

The two coupling strain energy terms $W_{x,xy}$ and $W_{xy,x}$ shown in Equation 13 can be used to characterize vibration coupling effects on damping. This is done by summing the contribution of coupling energy dissipation due to the two coupling strain energy terms; that is,

$$F_c = \sum_{k=1}^{n} [\eta^{(k)}_x\, W^{(k)}_{x,xy} + \eta^{(k)}_{xy}\, W^{(k)}_{xy,x}]/(\eta W_t) \quad (15)$$

where F_c characterizes the effects of vibration coupling on damping in terms of the fraction of coupling energy dissipation in the total energy dissipation. It should be noticed that different lamina loss factors are used in the two coupling strain energy terms to calculate the total coupling energy dissipation. This is because $W_{x,xy}$ is decomposed from the extensional strain energy W_x (Equation 7), and thus the extensional coupling energy dissipation is calculated based on the extensional loss factor η_x. On the other hand, the in-plane shear loss factor η_{xy} is used for calculating the coupling energy dissipation due to $W_{xy,x}$, which is decomposed from the in-plane shear strain energy W_{xy} (Equation 8).

4. Finite element model

The finite element code used in this work was the SAP IV program [20]. The finite element model used in this study was made of three-dimensional eight-node thick shell elements. A typical finite element model used in this study is shown in Fig. 1. The model used only one element in the laminate width direction. This was based on a displacement study for 12-ply symmetric laminates with three elements in both the length and width directions. It was found that, although the resulting transverse displacements (in the thickness direction) varied drastically along the length direction, they remained nearly constant along the width direction. This is because the model was made of a 12-ply thin laminate with a low width-to-thickness ratio (i.e. laminate having dimensions of 20.32 cm length × 1.905 cm width × 0.152 cm thickness). The distance between two adjacent nodes along the width direction was so small that not much variation in transverse displacements was observed between the two adjacent nodes. Thus, only one element is needed to model the laminate width dimension. However, in order to account for material discontinuity along the laminate thickness such as in the case of the antisymmetric laminates, two elements were used in the laminate thickness direction with each element representing six laminae (lamina thickness = 0.127 mm) of the same fibre orientation (Fig. 1). Such a simplification is only appropriate for thin laminates. For thick laminates, more elements need to be introduced in the laminate thickness direction [11, 12].

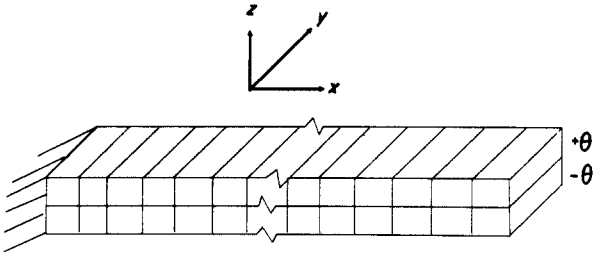

Figure 1 A typical finite element model for 12-ply graphite–epoxy laminated cantilever beams.

The number of elements used in the length direction was determined based on a strain energy convergence study [10]. The finite element model was started with a network of large elements, and the element size was reduced to determine the required element size for convergence. Accordingly, the final finite element model that was selected in this work consists of 520 elements, which resulted in a total of 1560 nodes with 4602 degrees of freedom. This model was used in both the symmetric and antisymmetric laminates in order to maintain the same element aspect ratio in both laminates. The finite element program was used to predict resonant frequencies and mode shapes, and since the program does not have the capability for calculating strain energy and damping, a modification of the program was required. This involves a Gaussian quadrature numerical integration for strain energy based on the resulting mode shapes. For a detailed description of the strain energy integration, the reader is referred to Hwang [19].

5. Results and discussion

A free-vibration modal analysis was performed on graphite–epoxy cantilever beams with two stacking sequences: (i) 12-ply symmetric laminates [12(θ)], and (ii) 12-ply antisymmetric laminates [6(θ)/6(− θ)]. Material properties in principal material directions used as input data to the finite element analysis were adapted from previous work [10, 19]. The fibre orientation was varied from 0° to 90° to study the effects of fibre orientation on vibration coupling and damp-

ing. It was found that only three of the resulting six stress components contributed greatly to the total damping. These three major stress components are the longitudinal normal stress (or bending stress, σ_x), the in-plane shear stress (τ_{xy}) and the interlaminar shear stress (τ_{xz}). The energy dissipation due to these three stresses was further decomposed to identify the coupling energy dissipation. Table I shows the resulting contributions of the three major stress components. The results are presented based on the first three modes including two flexural modes and one torsional mode, which were defined based on the resulting mode shapes.

According to the definition by Adams and Bacon [6], a laminate is said to be in "free flexure" when it is subjected to pure bending and any resulting twisting. On the other hand, a laminate is said to be in "pure flexure" when it is subjected to a pure bending, and the twisting is prevented by constraints [6]. Thus, except for the case of 0° and 90° laminates, none of the resulting modes were in pure flexure or pure torsion. In fact, they were in either free flexure or free torsion. This is because the modes were coupled with bending and twisting due to the coupling stiffness $\bar{C}_{16}$. As shown in the second column of Table I, 1F and 2F represent the first and the second flexural modes, respectively, and 1T is the first torsional mode. This notation will also be used later in the figures for the purpose of presenting the results. The distinction between flexural and torsional modes was made according to the resulting mode shapes. For example, for a flexural mode, the resulting transverse displacement data along the flexural direction of interest must have the same sign (although the amount may be different due to the effects of coupling) over any cross-section of the laminate. On the other hand, a torsional mode is evidenced by the different signs of such transverse displacement data on opposite sides of the beams. Accordingly, for laminates with fibre orientation other than 0°, the first two modes were found to be in flexure, and the third mode was found to be in torsion. However, for the case of 0° laminates, the second mode was found to be in torsion, and both the first and third modes were found to be in flexure.

According to the results shown in Table I, the contribution of damping for the first flexural mode is dominated by the bending stress σ_x. This was expected, since the first mode is essentially in bending, and most of the strain energy stored in the laminate would be dominated by the bending strain energy. The difference in the contribution of damping between the two laminate models is that the contributions of damping such as F_x and F_{xz} for the symmetric laminates are always higher than those of antisymmetric laminates. In contrast, the contribution of damping F_{xy} due to the in-plane shear stress in antisymmetric laminates is considerably higher than that of symmetric laminates. This is because more in-plane shear strain energy was generated in antisymmetric laminates due to discontinuity in material properties between the laminae.

In the case of antisymmetric laminates, the three major components of damping for the second flexural mode do not show as much difference as those of the first flexural modes. This was not observed in the case of symmetric laminates. Instead, a drastic increase of the contribution of in-plane shear stress (F_{xy}) was found in symmetric laminates. This is probably due to the fact that more in-plane twisting strain energy was generated in the second mode since the two flexural

TABLE I Contribution of damping due to the three major stress components τ_{xz}, σ_x and τ_{xy}.

θ (deg)	Mode No.	[12(θ)]			[6(θ)/6(−θ)]		
		F_{xz} (%)	F_x (%)	F_{xy} (%)	F_{xz} (%)	F_x (%)	F_{xy} (%)
0	1F	27.2	72.8	0.0	27.2	72.8	0.0
	1T	1.3	0.6	98.1	1.3	0.6	98.1
	2F	34.7	65.3	0.0	34.7	65.3	0.0
15	1F	10.1	81.4	8.4	3.0	51.5	45.4
	2F	3.7	46.9	49.4	3.2	50.8	45.9
	1T	3.6	10.9	85.4	0.7	23.0	73.6
30	1F	11.4	78.1	10.4	2.6	60.9	36.3
	2F	4.0	60.9	35.1	2.8	60.9	36.2
	1T	3.7	59.1	37.2	0.6	34.8	55.0
45	1F	15.9	75.8	8.1	4.1	62.5	33.1
	2F	6.3	63.0	35.6	4.3	62.7	32.8
	1T	6.0	62.3	31.7	0.7	24.3	51.3
60	1F	19.7	76.0	4.1	8.3	61.7	29.6
	2F	11.7	64.3	23.9	8.6	61.5	29.4
	1T	11.1	62.9	25.9	8.9	61.3	29.3
75	1F	20.1	79.1	0.7	17.0	70.9	11.7
	2F	18.6	74.0	7.3	17.8	70.0	11.8
	1T	0.0	98.5	1.3	0.0	99.2	0.7
90	1F	19.2	80.8	0.0	19.2	80.8	0.0
	2F	20.1	79.8	0.0	20.1	79.8	0.0
	1T	0.0	98.9	1.0	0.0	98.9	1.0

modes are not in pure flexure. Thus, an increase in the contribution of in-plane shear stress to damping was found in the second flexural mode, while the other two components were reduced. For the case of the torsional mode, it appears that both the bending stress, σ_x, and in-plane shear (or twisting) stress, τ_{xy}, contributed greatly to the total energy dissipation as compared with the interlaminar shear stress, τ_{xz}. The contribution of the in-plane shear stress to damping is maximized at 0°, and it then decreases with increasing fibre angle. On the other hand, the contribution of bending stress to damping is a minimum at 0°, and it then increases up to a maximum at 90° with increasing fibre orientation.

Since the contribution of damping was dominated by the three major stress components, the resulting three strain energy terms were further decomposed to identify the associated coupling strain energy and to study its effect on damping. Figs 2 and 3 show the resulting coupling contribution to damping as a function of fibre angle for symmetric and antisymmetric laminates, respectively. For the case of symmetric laminates, the coupling contribution is dominated by the coupling between bending and twisting. On the other hand, the coupling contribution to damping in antisymmetric laminates is governed by the coupling between bending and extension. As expected, no coupling contribution is made at the fibre angle of 0° and 90° in either laminate model. It appears that the two flexural modes exhibited similar distributions, with a maximum coupling contribution at a fibre angle around 30°. Similar results were also obtained by other investigators. For example, Adams and Bacon [6] indicated that the damping peak near a fibre angle of 30° is associated with the lamina coupling stiffness $\bar{C}_{16}$. However, no attempt was made to investigate the contribution of such a coupling to the total damping. In the present work, the effects of coupling on damping is investigated in terms of the ratio of coupling energy dissipation to the total energy dissipation using the decomposition approach. Since the value of $\bar{C}_{16}$ is maximized at 30°, a maximum coupling strain energy is generated at that angle, which in turn resulted in a maximum coupling energy dissipation.

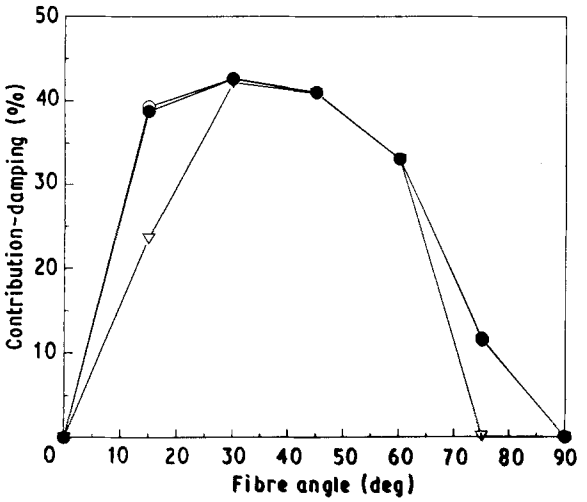

Figure 2 Contribution of damping due to bending–twisting coupling with respect to fibre angle for symmetric graphite–epoxy laminates, [12(θ)]: (○) Mode 1F, (●) Mode 2F, (▽) Mode 1T.

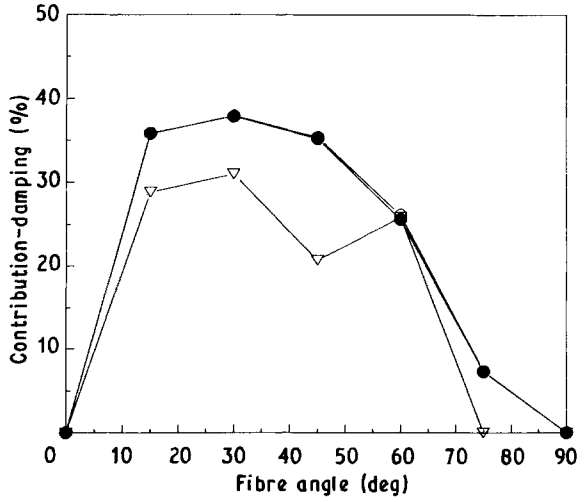

Figure 3 Contribution of damping due to bending–extensional coupling with respect to fibre angle for antisymmetric graphite–epoxy laminates, [6(θ)/6(− θ)]: (○) Mode 1F, (●) Mode 2F, (▽) Mode 1T.

For the case of torsional modes, the coupling contribution is generally lower than those of the two flexural modes. The contribution of bending–twisting coupling to damping in symmetric laminates decreases to zero at 75°, which is different from that of the two flexural modes. For the case of antisymmetric laminates, although the maximum coupling contribution in the torsional mode was found to be at a similar fibre angle as in the flexural modes, a discontinuity in coupling contribution to damping was found at a fibre angle around 45°. This is probably because of the increase of the non-coupling strain energy due to the increase of torsional stiffness at that fibre angle. As will be shown later, the torsional frequency is maximized at a fibre angle around 45° for the case of antisymmetric laminates, because of the maximum torsional stiffness at that fibre angle. On the whole, it appears that the contribution of damping due to bending–twisting coupling in symmetric laminates is higher than that due to bending–extensional coupling in antisymmetric laminates.

Figs 4 and 5 show the resulting total loss factor data as a function of fibre orientation for symmetric and antisymmetric laminates, respectively. The loss factor for the two flexural modes appears to increase with increasing fibre angle up to a maximum at a fibre angle near 30°. This is because a maximum coupling effect occurs at that fibre angle. It then gradually decreases with increasing fibre angle. Similar results were also reported by Adams and Bacon [6]. In both laminate models, the resulting loss factors for the torsional mode were higher than those of the two flexural modes. This was expected, since more twisting energy dissipation is generated in the torsional mode. It should be mentioned that, although the maximum coupling contribution in the torsional mode occurred at a fibre angle around 30°, the maximum loss factor, however, was found at the fibre angle of 0°. This is because the total torsional energy dissipation consists

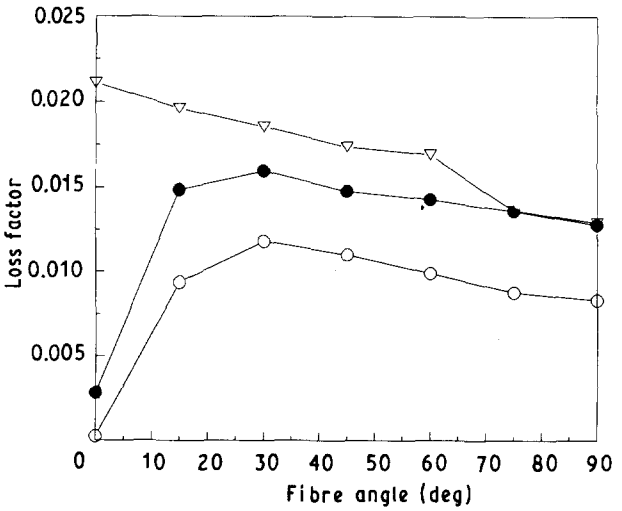

Figure 4 Variation of total loss factor with fibre angle for symmetric graphite–epoxy laminates, [12(θ)]: (○) Mode 1F, (●) Mode 2F, (▽) Mode 1T.

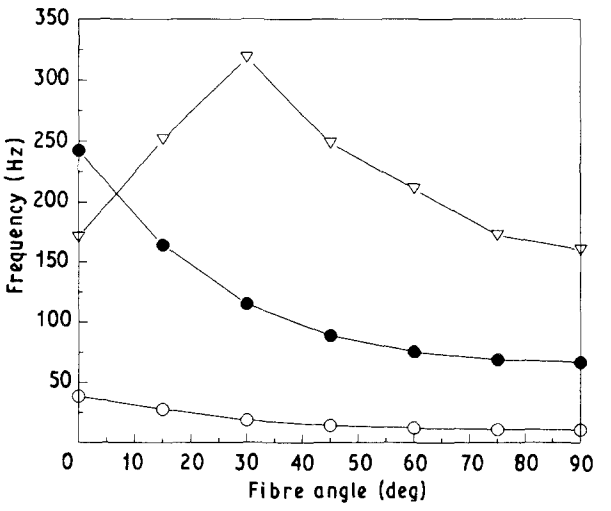

Figure 6 Variation of resonant frequency with fibre angle for symmetric graphite–epoxy laminates, [12(θ)]: (○) Mode 1F, (●) Mode 2F, (▽) Mode 1T.

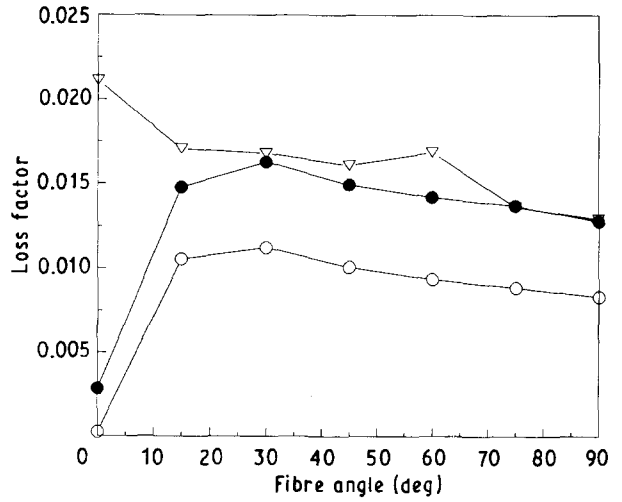

Figure 5 Variation of total loss factor with fibre angle for antisymmetric graphite–epoxy laminates, [6(θ)/6(− θ)]: (○) Mode 1F, (●) Mode 2F, (▽) Mode 1T.

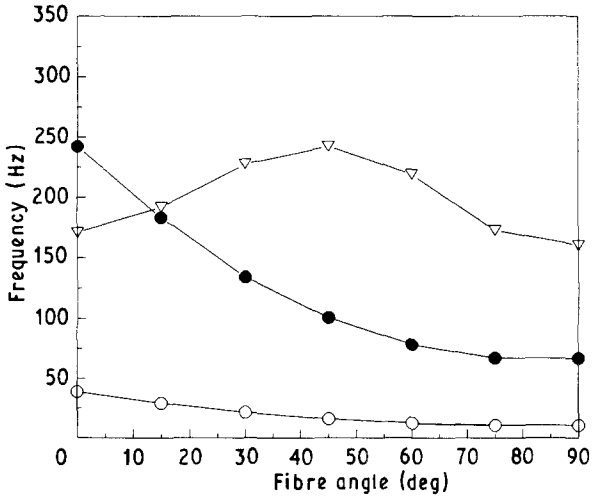

Figure 7 Variation of resonant frequency with fibre angle for antisymmetric graphite–epoxy laminates, [6(θ)/6(− θ)]: (○) Mode 1F, (●) Mode 2F, (▽) Mode 1T.

of non-coupling and coupling energy dissipation, and the non-coupling energy dissipation has a more significant contribution to damping. Thus, although there is no coupling energy dissipated in the 0° laminates, a maximum loss factor still exists at 0°.

Figs 6 and 7 show the variation of resonant frequency with fibre orientation for symmetric and antisymmetric laminates, respectively. The resulting frequency data for the two flexural modes generally exhibited similar distributions. That is, the frequency decreases with increasing fibre orientation. This is due to the fact that the flexural stiffness of the beam decreases with increasing fibre orientation, and lower frequencies are generated as the flexural stiffness decreases. The frequency distributions for the torsional mode, however, are not as smooth as those of the two flexural modes. For example, in the case of symmetric laminates, the frequency of the torsional mode increases with increasing fibre orientation up to a maximum at a fibre angle around 30°, and it then decreases with increasing fibre orientation. This is probably because the combined effects of the bending–twisting coupling stiffnesses (A_{16} and D_{16}) in the torsional mode are maximized at that fibre angle. A similar trend occurred in the torsional mode of antisymmetric laminates, with a difference that the maximum torsional frequency was found at a fibre angle around 45°. It is again likely that the bending–extensional coupling stiffness (B_{16}) of the torsional mode is maximized due to a maximum torsional stiffness at that fibre angle.

6. Concluding remarks

A new method for characterizing the vibration coupling effects on damping of composite materials has been introduced. The application of this method to characterize the effects of bending–twisting coupling and bending–extensional coupling on damping in both symmetric and antisymmetric laminates has been demonstrated. A maximum coupling effect on damping was found at a fibre angle around 30° for the first three modes of vibration. The coupling effects tend to increase the vibration damping in the flexural modes.

The non-coupling energy dissipation was found to be more dominant for the flexural modes at a fibre angle of 90°. The non-coupling energy dissipation for torsional modes appears to be more dominant at a fibre angle of 0°, however. On the whole, the method described in this paper provides considerable potential for full three-dimensional analysis in the design and vibration control of composite materials and structures.

References

1. C. W. PRYOR Jr. and R. M. BARKER, *J. Compos. Mater.* **4** (1970) 549.
2. R. B. ABARCAR and P. F. CUNNIFF, *ibid.* **6** (1972) 504.
3. E. A. THORNTON and R. R. CLARY, "Composite Materials: Testing and Design (Third Conference)", ASTM STP 546 (American Society for Testing and Materials, Philadelphia, 1974) p. 111.
4. I. G. RITCHIE, H. E. ROSINGER and W. H. FLEURY, *J. Phys. D: Appl. Phys.* **8** (1975) 1750.
5. D. W. JENSEN, E. F. CRAWLEY and J. DUGUNDJI, *J. Reinf. Plast. Compos.* **1** (1982) 254.
6. R. D. ADAMS and D. G. C. BACON, *J. Compos. Mater.* **7** (1973) 402.
7. D. X. LIN, R. G. NI and R. D. ADAMS, *ibid.* **18** (1984) 132.
8. R. D. ADAMS and R. F. LAMBERT, in Proceedings of DAMPING 1986 Conference, Vol. 2, edited by L. Rogers, (1986) AFWAL-TR-86-3059 Paper No. FH-1.
9. S. J. HWANG and R. F. GIBSON, *J. Engng Mater. Technol.* **109** (1987) 47.
10. *Idem, Compos. Sci. Technol.* **41** (1991) 379.
11. *Idem*, in Proceedings of 5th Technical Conference on Composite Materials, East Lansing, Michigan, June 1990 (American Society for Composites) p. 26.
12. *Idem, Compos. Struct.* **20** (1992) 29.
13. P. R. MANTENA, R. F. GIBSON and S. J. HWANG, in Proceedings of DAMPING 89 Conference, West Palm Beach, Florida, February 1989, edited by L. Rogers, WRDC-TR-89-3116, Paper No. IAB.
14. *Idem, AIAA J.* **29** (1991) 1678.
15. S. J. HWANG and R. F. GIBSON, presented at Aeromat 90 Advanced Aerospace Materials Conference, Long Beach, California, May 1990.
16. *Idem, Compos. Sci. Technol.* **43** (1992) 159.
17. R. M. JONES, "Mechanics of Composite Materials" (Hemisphere, New York, 1975) pp. 154, 214.
18. S. A. SUAREZ and R. F. GIBSON, *J. Test Eval.* **15** (1987) 114.
19. S. J. HWANG PhD dissertation, University of Idaho, Moscow, Idaho (1988) pp. 16, 18, 60, 39.
20. K. J. BATHE, E. L. WILSON and F. E. PETERSON, "SAP IV–A Structural Analysis Program for Static and Dynamic Response of Linear Systems" (University of California, Berkeley, California, 1974).

Received 6 September 1991
and accepted 2 June 1992